

Enhanced adsorption of humic acid on APTES modified palygorskite: behavior and mechanism

Jiahong Wang^{a,b,*}, Shaochong Liu^a, Wei Tang^b

^aSchool of Environmental Science and Engineering, Shaanxi University of Science & Technology, Xi'an 710021, China, Tel. +86 029 8616 8291, email: wangjiahong@sust.edu.cn (J.H. Wang), 1042525313@qq.com (S.C. Liu)

^bShaanxi Research Institute of Agricultural Products Processing Technology, Xi'an 710021, China, Tel. +86 029 8616 8307, email: Tangwei@sust.edu.cn (W. Tang)

Received 2 August 2016; Accepted 12 April 2017

ABSTRACT

Aminopropyl triethoxysilane (APTES) modified palygorskite (PA-NH₂) was prepared and characterized by Fourier transform infrared spectroscopy, X-ray photoelectron spectroscopy, thermo gravimetric analysis and zeta potential tests, and its adsorption behavior for humic acid (HA) was studied. Characterized results suggested that aminopropyl group was successfully anchored on the surface of palygorskite. Maximum adsorption capacity of HA on PA-NH₂ is 71.43 mg/g at 25°C, which is remarkably higher than pure PA. HA adsorption on PA-NH₂ decreased monotonously with an increase of solution pH. The presence of Na⁺ and Ca²⁺ increased HA adsorption on the adsorbent by the neutralized electrostatic repulsion between HA molecules to be adsorbed and adsorbed. HA adsorption over PA-NH₂ could be well described by Freundlich model and the adsorption process obeyed pseudo-second order kinetics model. PA-NH₂ has good desorption capability in alkaline solution and can be recycled. XPS analysis demonstrates that HA adsorption on the PA-NH₂ is due to the formation of new complex by electrostatic attraction between protonated amino groups of the adsorbent and disassociated carboxyl and phenolic hydroxyl groups of HA molecules. The competitive adsorption of OH⁻ anions with negatively charged HA molecules for amino groups of the adsorbent led to the desorption of HA adsorbed on the adsorbent.

Keywords: APTES modified palygorskite; adsorption; desorption; humic acid

1. Introduction

The presence of humic acid (HA) in water may cause a great influence on the transport of toxic heavy metals and other organic pollutants by reacting with these matter, and membrane fouling during membrane separation process [1,2]. HA may also act as a nutrient of microorganism in drinking water distribution system. Furthermore, HA is also recognized as the major precursor of carcinogenic disinfecting byproducts formed in chlorinated drinking water [3–5]. Therefore, the development of effective treatment methods to eliminate HA from aqueous solution is of great importance.

Due to its simplicity and high efficiency, adsorption technique has attracted great attention for the removal

of HA from aqueous solution. Development of high efficiency and low cost adsorbent is the key to the success of adsorption method. Recently, natural mineral adsorbents were frequently developed for the elimination of aqueous HA because of their abundance and cost effectiveness. For example, zeolitic tuff [6], kaolinite [7,8], bentonite [9,10], montmorillonite [11], palygorskite [12], vermiculite/palygorskite [13], were used as an adsorbent for HA removal. Palygorskite (PA) is an aluminum-magnesium with fibrous morphology, which is abundant in China. Due to its physicochemical characteristics (high surface area and porosity, moderate ionic exchange capacity and chemical inertness), PA is highly valued for its adsorption properties. However, PA has permanent negative charges on its surface in aqueous solution, which may suppress its adsorption for the negatively charged HA molecules. Surface modifications of PA with inorganic or organic reagents may augment the

*Corresponding author.

adsorption performance for aqueous HA. Aminated adsorbents including aminated polyacrylonitrile fibers [14], chitosan [15,16], amine functionalized magnetic mesoporous composite microspheres [17], amine-modified polyacrylamide–bentonite composite [18], magnetic separable polyaniline [19], have been found to be efficient to remove HA from aqueous solution. Therefore, amino-functionalization of PA may improve its adsorption for HA, for example, polyaniline modified attapulgite composite showed high adsorption capacity for aqueous HA [20]. Nevertheless, to our best knowledge, no studies have been conducted to develop the aminopropyltriethoxysilane (APTES) modified PA for the removal of HA from aqueous solution.

In this study, APTES modified PA (PA-NH₂) was prepared and characterized by Fourier transform infrared spectroscopy (FTIR), X-ray photoelectron spectroscopy (XPS), thermo gravimetric analysis (TGA) and zeta potential measurement. The adsorption and desorption characteristics of PA-NH₂ for HA in aqueous solution were evaluated by batch experiments. The possible adsorption and desorption mechanism of HA on the adsorbent was also advised.

2. Materials and methods

2.1. Materials

The raw PA with an average particle size of 300 mesh screen used in this work was purchased from Jiangsu Hui Da Mining Technology Co. Ltd. Humic acid sodium and 3-aminopropyltriethoxysilane (APTES) were supplied from Aldrich Company. Other chemicals purchased from Sino-pharm Chemical Reagent Co. Ltd., China were of analytical grade and used without further purification.

2.2. Preparation of PA-NH₂

The raw PA was purified by acid treatment. Briefly, 20 g raw PA was dispensed in 200 ml of distilled water and sonicated for 30 min. The large solids in the bottom were removed. PA after sonication treatment was added to 200 ml of 1 mol/L HCl with constant stirring for 8.5 h to remove carbonate and adsorbed cations. The solids were filtered and washed with distilled water until neutral pH, followed by drying at 105°C under vacuum for 12 h. To prepare PA-NH₂, 4.0 g purified PA was dispensed in 250 ml three-necked flask with 160 ml of toluene and sonicated for 30 min. Then 6 ml of APTES was added to the flask, and the mixture was refluxed at 110°C with constant stirring for 12 h under a nitrogen flow (40 ml/min). The resulting solids were filtered and washed by ethanol extraction for 12 h to remove the unreacted APTES, followed by drying at 70°C for 12 h under vacuum conditions.

2.3. Adsorbent characterization

The FTIR spectra of PA and PA-NH₂ were recorded on a Vector-22 FTIR spectrometer (Bruker, Germany) with the KBr pellet technique. XPS (Perkin Elmer PHI 550 ESCA/SAM, USA) equipped with a monochromatized AlK α X-ray radiation at 1486.6 eV was used to analyze the surface properties of the samples. TGA curves of two samples were

conducted using a Perkin–Elmer Pyris 1 TGA instrument (Perkin–Elmer, USA) from 25 to 600°C under N₂ at a heating rate of 10°C/min. Zeta potentials of PA and PA-NH₂ were determined on a zeta potential analyzer (Brookhaven, USA).

2.4. Adsorption experiments

The batch experiments were conducted to determine the adsorption isotherm of HA on PA-NH₂. In detail, 20 mg PA-NH₂ was placed in Teflon capped glass tube receiving 40 ml of HA solution with the initial concentration at 15.8–157.5 mg/L and pH 6.6–7.0. The mixture was transferred into an incubator and shaken at 160 rpm. After achieving to adsorption equilibrium, the adsorbents were filtered from the aqueous solution and residual concentration of HA were tested by a UV-vis spectrophotometer at 254 nm wavelength. The amount of HA adsorbed on the adsorbent were calculated based on the difference of the initial and residual concentration of HA in aqueous solution.

To determine the effect of contact time on HA adsorption on the adsorbents, 200 mg PA-NH₂ were dispensed in 500 ml three-necks flask containing 400 ml HA solution with the initial HA concentration with 31.5, 63.0 and 126.0 mg/L, respectively, at pH 6.8–7.0. The mixture was stirred continuously, and at the predetermined interval, 4 ml of the mixture was withdrawn and filtered. The concentration of HA in the supernatant at different time intervals was determined spectrophotometrically.

The effect of solution pH on HA adsorption onto PA-NH₂ was investigated by dispensing 20 mg PA-NH₂ in 40 ml of 63.0 mg/L HA solution at pH range of 2–10. The different solution pH was adjusted by 0.1 mol/L NaOH and HCl solution. For the effect of cations, 20 mg PA-NH₂ was dispensed in 40 ml HA solution with initial HA concentration at 15.8–157.5 mg/L and Na⁺ concentration of 5 mmol/L or Ca²⁺ concentration of 0.5 mmol/L and pH 6.6–7.0. The effect of ionic concentration on HA adsorption onto the adsorbent was also conducted. Briefly, 20 mg PA-NH₂ was added into 40 ml of 63.0 mg/L HA solution with ionic concentration of Na⁺ and Ca²⁺ at 0.25–10 mmol/L and pH 6.7–6.9.

2.5. Regeneration of the adsorbent

To determine the desorption and regeneration property of the adsorbent, 20 mg PA-NH₂ was added to 40 ml of 82.16 mg/L HA solution. After reaching adsorption equilibrium, HA saturated PA-NH₂ was separated and re-dispensed into 20 ml of 0.01 mol/L NaOH solution and shaken at 160 rpm for 10 h. The adsorbent was separated centrifugally and washed with deionized water for three times. The regenerated adsorbent was explored for the removal of HA in subsequent cycles.

3. Results and discussion

3.1. Adsorbent characterization

The FTIR spectra of PA and PA-NH₂ are shown in Fig. 1. From the results, several new bands were seen on the spectrum of APTES modified PA. The bands at 694, and 1471 cm⁻¹ are ascribed to the stretching and bending vibrations

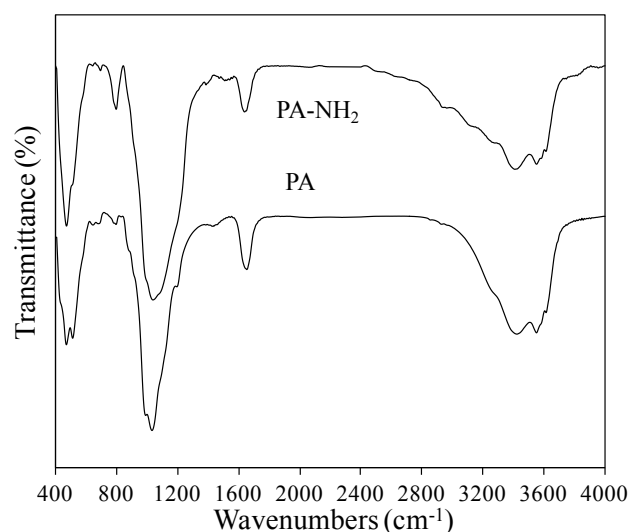


Fig. 1. FTIR spectra of PA and PA-NH₂.

of amino group on the surface of the adsorbent. The bands at 1386 and 2930 cm⁻¹ are assigned to the C–H stretching vibration of the CH₂ in alkyl chain on the surface of PA [21]. The results indicate that PA has been successfully modified by aminopropyl silane coupling agents. The similar results were obtained for XPS survey spectra of PA and PA-NH₂ (in Fig. S1). From the plot, the presence of the elements such as Si, Al, Mg, C and O in two samples was observed, which are the typical elements of PA. For PA-NH₂, a new peak at binding energy about 400 eV assigned to N1s was appeared and the atom ratio of N element was 4.07%, which again confirms the successful modification of PA with APTES.

The TGA curves of PA and PA-NH₂ are shown in Fig. 2. From the results, the obvious weight losses at temperature below 200°C were observed for two samples, which is ascribed to the surface adsorbed water and zeolite water on the surface of PA and PA-NH₂ [22]. The weight loss of 4.31% at temperature of 200–580°C in PA is assigned to the departure of constitutional water. For PA-NH₂, the weight loss of 7.35% at temperature of 200–580°C is attributed to the decomposition of aminopropyl group on the PA surface and the loss of constitutional water. By subtracting the weight loss of lattice water, the weight percent of aminopropyl group on the surface of PA-NH₂ is 3.04%. Zeta potentials of PA and PA-NH₂ are shown in Fig. S2. It was observed that the isoelectric points (IEP) of PA and PA-NH₂ were at pH 1.95 and 5.80, respectively. Surface modification of PA with APTES greatly improves the IEP of PA, which is beneficial for the adsorptive removal of negatively charged HA molecules in aqueous solution.

3.2. Adsorption experiments

3.2.1. Effect of solution pH

Effect of solution pH on the amount of HA adsorbed onto PA-NH₂ is shown in Fig. 3. From the result, the amount of HA adsorbed on the adsorbent decreases continuously with an increase of solution pH, and the obvious declining trend is observed at pH above 6.2. This may be attributed to

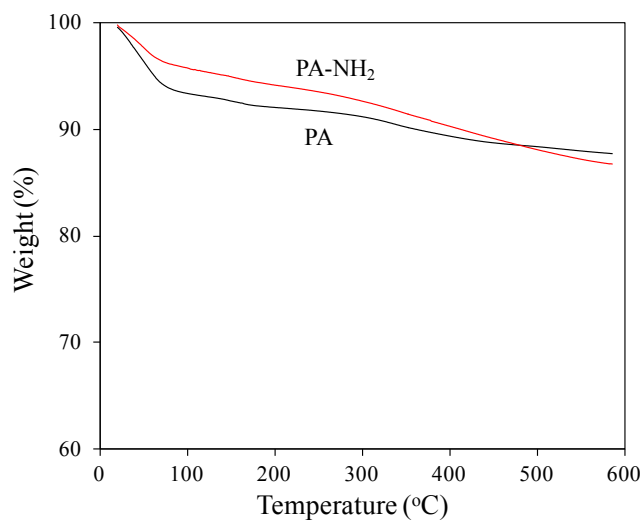


Fig. 2. TGA curves of PA and PA-NH₂.

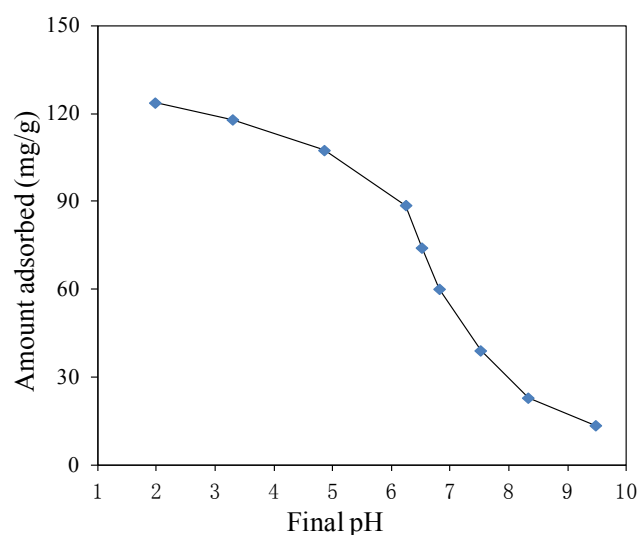


Fig. 3. Effect of solution pH on HA adsorption onto PA-NH₂.

the changes of physicochemical properties of HA molecules and the adsorbent. HA molecules are negatively charged because of the dissociation of carboxyl groups and phenolic groups at pH above 1.9 [20]. Whereas amino groups of PA-NH₂ particles are protonated at pH below 9.8 [23], invoking the electrostatic attraction between HA molecules and the protonated amino groups of adsorbent, which results in the effective adsorption of HA on PA-NH₂. At low pH (below 3), the structure of HA molecules becomes more spherical and can form tiny aggregates, which may result in HA flocculation, leading to enhanced HA adsorption [15,24]. With increasing solution pH, the decreased protonation of aminopropyl group would weaken the electrostatic attraction with HA molecules, which resulted in the decreased HA adsorption on the adsorbent. In addition, the IEP of PA-NH₂ is at pH 5.8, which is co-determined by the hydroxyl group and aminopropyl group on the surface of PA-NH₂. The

adsorbent would carry the negative charges at pH above 5.8, inducing the electrostatic repulsion between the adsorbent and negatively charged HA molecules, which accounts for the significant decrease of HA adsorption on PA-NH₂. The low amount of HA adsorbed on the adsorbent at high pH suggests that hydrogen bonding and van der Waals forces between PA-NH₂ and HA may also play a role in the HA adsorption. However, the electrostatic interaction is superior to hydrogen bonding interaction for HA adsorption.

3.2.2. Effect of background ions

Background ions are generally present in water, hence it is necessary to study the effect of Na⁺ and Ca²⁺ on HA adsorption. The impact of background ions on HA adsorption onto PA-NH₂ was conducted by addition of Na⁺ and Ca²⁺ in different concentration of HA, and the results were shown in Fig. 4a. From the results, the presence of Na⁺ and Ca²⁺ substantially increased the amount of HA adsorbed and the impact of Ca²⁺ is more obvious than that of Na⁺.

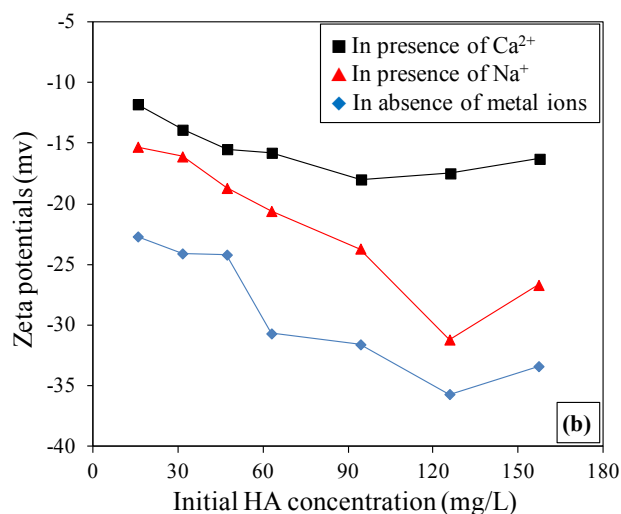
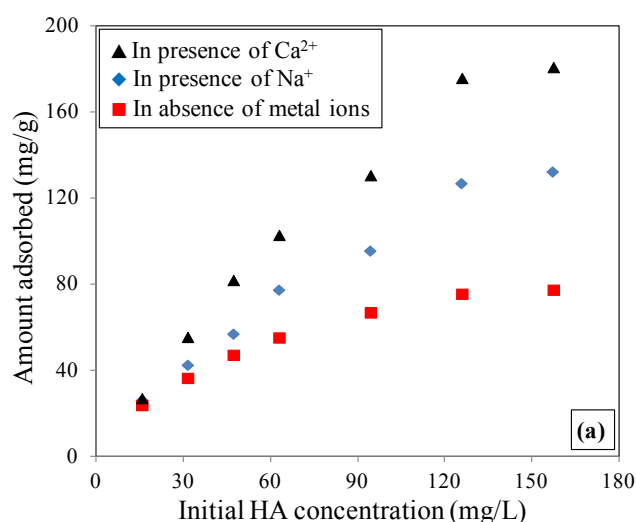


Fig. 4. Effect of Na⁺ and Ca²⁺ on HA adsorption onto PA-NH₂ (a) and zeta potentials of HA at different concentration (b).

The impact of Na⁺ and Ca²⁺ with different concentration on HA adsorption on the adsorbent was also studied, and the results are plotted in Fig. S3. For the effect of Na⁺, the amount of HA adsorbed on PA-NH₂ increased with increasing concentration of Na⁺. The continuous increase with increasing Ca²⁺ concentration was observed at initial concentration of Ca²⁺ below 2 mmol/L and gradually became stable with further increase of Ca²⁺ concentration. The enhanced HA adsorption in presence of Na⁺ and Ca²⁺ may be explained by the varying zeta potentials both in presence and absence of cations. As illustrated in Fig. 4b, the presence of Na⁺ and Ca²⁺ in the HA solution increases the zeta potential of HA in all initial HA concentration, which indicates that the addition of Na⁺ and Ca²⁺ neutralizes the negative charges of HA molecules. The neutralization decreases the electrostatic repulsion between HA molecules in solution and adsorbed, leading to the enhanced HA adsorption. Moreover, the shape of HA molecules may become coiled and spherical, which improved the mass transfer of HA molecules and enhanced HA adsorption [25]. Another reason may be attributed to the re-adsorption of HA molecules by interacting with the cations directly reacted with HA molecules adsorbed on the adsorbent [26]. The strong dependence of HA adsorption onto PA-NH₂ on solution pH and ionic strength also suggested that electrostatic interaction was the main adsorption mechanism.

3.2.3. Adsorption isotherms

Langmuir and Freundlich models are frequently adopted for the equilibrium adsorption process of organic and inorganic pollutions on adsorbents. Langmuir model and Freundlich model can be followed as:

Langmuir model:

$$q_e = \frac{q_m b C_e}{1 + b C_e} \quad (1)$$

Freundlich model:

$$q_e = K_f C_e^{\frac{1}{n}} \quad (2)$$

where q_e (mg/g) is the equilibrium amount adsorbed, C_e (mg/L) is the equilibrium concentration of HA, q_m (mg/g) is the theoretical saturation capacity, b (L/mg) is the affinity coefficient, K_f is Freundlich constant and $1/n$ is the heterogeneity factor.

Adsorption isotherm of HA on PA-NH₂ at 25°C is shown in Fig. 5 and the simulated parameters calculated from Langmuir model and Freundlich model are tabulated in Table S1. From Fig. 5, the amount of HA adsorbed on PA-NH₂ increases with increasing equilibrium HA concentration and the maximum amount of HA adsorbed on the adsorbent is 77.28 mg/g in tested range, which is far higher than that of raw PA [20], indicating that amino group on the adsorbent accounts for the enhanced HA adsorption. From Table S1, the correlation coefficient (R^2) for Freundlich model (0.992) is higher than that of Langmuir model (0.941), which indicates that HA adsorption on the adsorbent can be better described by Freundlich model than Langmuir model. It is inferred from the isotherm analysis that the adsorption of HA on the aminated adsorbent is a process built by cooper-

ation of more than one mechanisms like electrostatic interactions, hydrogen bonding and van der Waals forces. Since HA has a complex macromolecular structure, more than one kind of interactions can take role in its adsorption to

PA-NH₂. The calculated value of heterogeneity factor is less than one, indicating a beneficial process for the adsorption of HA on PA-NH₂.

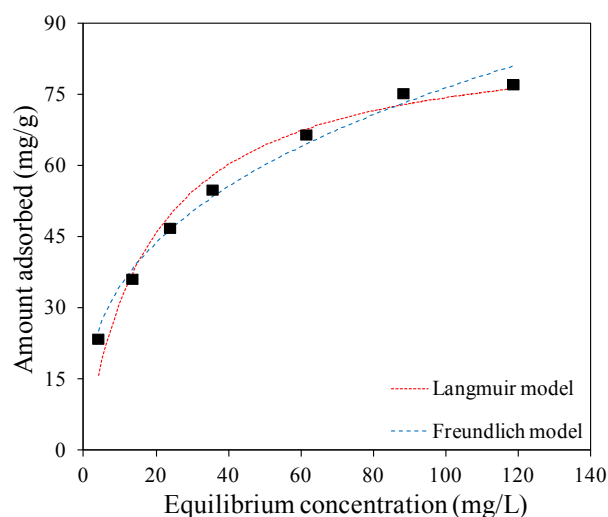


Fig. 5. Isotherm of HA adsorption on PA-NH₂ at pH 6.6~7.0 and 25°C.

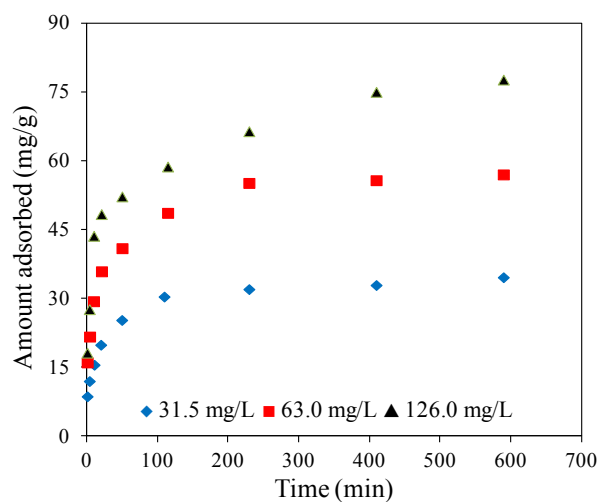


Fig. 6. Adsorption kinetics of HA on PA-NH₂ with initial HA concentration of 31.5, 63.0 and 126.0 mg/L, respectively, at pH 6.8~7.0 and 25°C.

3.2.4. Adsorption kinetics

The pseudo-second order and pseudo-first order model are frequently used to follow the mass transfer process of heterogeneous adsorption. The pseudo-first order kinetic and pseudo-second kinetic model can be expressed as follows:

Pseudo-first-order kinetic equation:

$$\log(q_e - q_t) = \log q_e - \frac{k_1}{2.303} t \tag{3}$$

Pseudo-second-order kinetic equation:

$$\frac{t}{q_t} = \frac{1}{k_2 q_e^2} + \frac{1}{q_e} t \tag{4}$$

where q_e (mg/g) is the amount adsorbed at equilibrium, q_t (mg/g) is the amount adsorbed at time t (min), k_1 (1/min) and k_2 (g/mg·min) are the pseudo-first-order rate constant and pseudo-second-order rate constant, respectively.

Effect of contact time on HA adsorption on PA-NH₂ at initial HA concentration of 31.5, 63.0 and 126.0 mg/L is illustrated in Fig. 6 and the simulated parameters of HA adsorption on the adsorbent are tabulated in Table 1. From the results, the correlation coefficients (R^2) calculated from the pseudo-second order kinetic is higher than that of pseudo-first order kinetic, and the calculated theoretical adsorption capacity of HA are almost identical to the experimental data, which indicates that the pseudo-second order kinetic is better than pseudo-first order kinetic to follow the HA adsorption process on the adsorbent and HA adsorption behavior is chemical adsorption. In addition, the adsorption rate constants (k_2) with the initial HA concentration of 31.5, 63.0 and 126.0 mg/L are 2.02×10^{-3} , 1.36×10^{-3} and 6.4×10^{-4} g/(mg·min), respectively, suggesting of a rapid HA adsorption at low initial HA concentration. This may be because that HA molecules at low concentration are easily bounded to the active sites of the adsorbent.

3.3. Regeneration of the adsorbent

Regenerability is an important factor to evaluate the reusability of the adsorbent. It is well known that alkaline conditions favor dissolution of HA in aqueous media. For

Table 1

Simulated parameters using pseudo-first order and pseudo-second order kinetics for HA adsorption onto PA-NH₂ at initial HA concentration of 31.5, 63.0 and 126.0 mg/L, respectively

C_0 (mg/L)	q_e (mg/g)	pseudo-first-order kinetic			pseudo-second-order kinetic		
		k_1 (min ⁻¹)	$q_{e,cal}$ (mg/g)	R^2	k_2 (g/mg·min)	$q_{e,cal}$ (mg/g)	R^2
31.5	34.62	4.61×10^{-3}	17.66	0.929	2.02×10^{-3}	35.71	0.998
63.0	57.00	9.21×10^{-3}	29.99	0.963	1.36×10^{-3}	58.82	0.999
126.0	77.67	9.21×10^{-3}	55.08	0.908	6.4×10^{-4}	83.33	0.995

this reason, 0.01 mol/L NaOH solution was thought to be a good desorption agent. Another benefit of NaOH may be replacement of humic macromolecules adsorbed through electrostatic interactions by the effect of hydroxide ions. The desorption and regeneration cycles was conducted for four times and the results are illustrated in Fig. 7. From the results, the slight decrease of the amount adsorbed of HA on the regenerated adsorbent was observed in first and second desorption-regeneration cycles and no obvious decrease of HA adsorption was found in next two desorption-regeneration cycles. After four desorption-regeneration cycles, the amount of HA adsorbed on the adsorbent reduced from

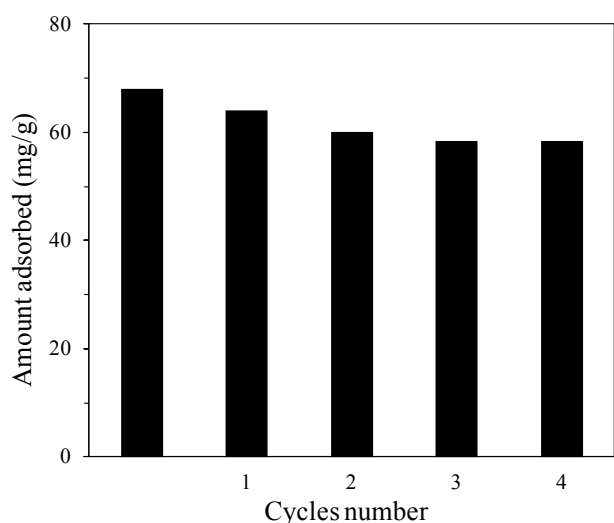


Fig. 7. Amount adsorbed of HA on regenerated PA-NH₂ adsorbent.

68.0 to 58.4 mg/g. Results suggested that the regenerated PA-NH₂ still showed high adsorption capacity for aqueous HA and the adsorbent can be used repeatedly.

3.4. Adsorption and desorption mechanism

Since aminopropyl group anchored on the surface contributed to the augmented HA adsorption, high resolution XPS spectra of C1s and N1s were applied to describe the adsorption and desorption mechanism of HA on PA-NH₂. The C1s spectra of PA-NH₂ before HA adsorption, after HA adsorption and after HA desorption are illustrated in Fig. 8a. For PA-NH₂, C1s spectrum can be decomposed into three single peaks with assignments at 284.8 eV as C–C, 286.1 eV as C–O or C–N, and 288.6 eV as C=O, indicating the successful modification of PA with APTES. The presence of C=O peak may be attributed to hydrocarbon contamination on the surface [21,27]. After HA adsorption on the adsorbent, the contribution of C=O increased from 1.73% to 8.49%, which is ascribed to the carboxyl group of HA molecules, suggesting that HA molecules have been anchored on the surface of the adsorbent. For the regenerated adsorbent, the contribution of C=O was 2.19%, which indicates that HA molecules on the adsorbent have been desorbed in alkaline solution. It is notable that the contribution of C=O peak after HA desorption is higher than that before HA adsorption, indicating that there are still a few HA molecules bound to the adsorbent, which may be the reason for the reduced HA adsorption on the regenerated adsorbent. The similar results are observed in N1s spectra (in Fig. 8b). As illustrated in Fig. 8b, the N1s peak can be divided into two single peaks at binding energy of 399.3 and 401.5 eV, ascribed to the free amino group (–NH₂) and the protonated amino group (–NH₃⁺). The presence of the protonated amino

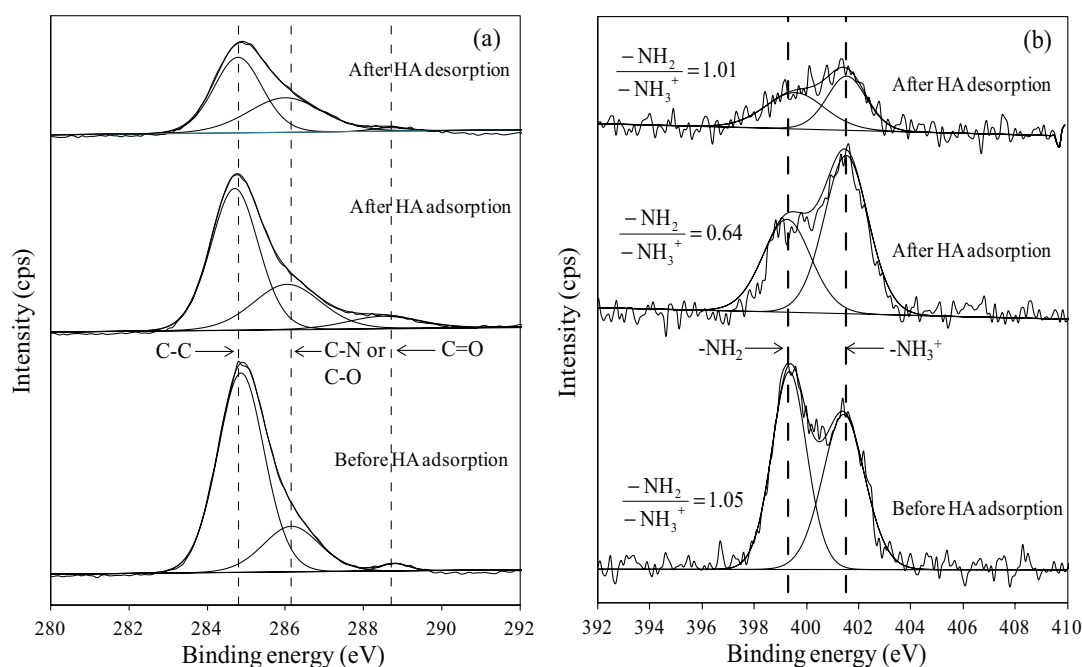


Fig. 8. XPS C1s (a) and N1s (b) spectra of PA-NH₂ before HA adsorption, after HA adsorption and after HA desorption.

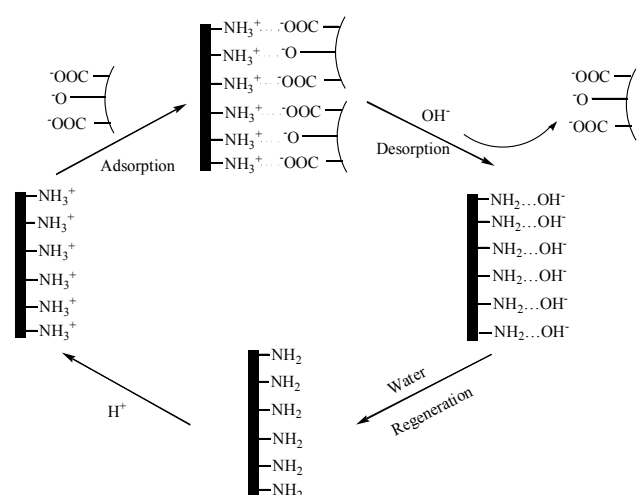


Fig. 9. Schematic mechanism for HA adsorption and desorption on PA-NH₂.

group is due to the interaction between the free amino group and free hydroxyl group on the surface of PA during the silylation process [28, 29]. After HA adsorption, the similar two peaks were observed, whereas the content ratio of $-NH_2$ to $-NH_3^+$ decreased from 1.05 to 0.64, which indicated that HA molecules have been complexed with free amino groups on the surface of the adsorbent. After HA desorption, the content ratio of $-NH_2$ to $-NH_3^+$ increased to 1.01, indicating the deprotonation of $-NH_3^+$ during the desorption process. Compared with the adsorbent before HA adsorption, the lower content ratio of $-NH_2$ to $-NH_3^+$ after HA desorption is also reflecting the incomplete desorption of HA molecules from the adsorbent.

Based on this study, the possible schematic mechanism for HA adsorption and desorption on PA-NH₂ was advised (in Fig. 9). During HA adsorption, free amino group on the surface of the adsorbent was protonated in HA solution, which induced the strong electrostatic attraction with the carboxyl group and phenolic hydroxyl group of HA molecules to form a new complex, leading to the enhanced HA adsorption on the adsorbent. When HA loaded adsorbent was desorbed in alkaline solution, the protonated amino group on the adsorbent would be deprotonated and OH⁻ anions in solution would be competed with negatively charged HA molecules and bounded to the amino group of the adsorbent, therefore resulting in desorption of HA molecules.

4. Conclusion

Due to its large specific surface area and cost effectiveness, PA was modified with APTES groups and used as an effective adsorbent for the removal of HA from aqueous solution. APTES modified PA exhibits substantially higher adsorption capacity for HA than raw PA. The enhanced HA adsorption can be attributed to form the new complex between HA molecules and the amino groups of the adsorbent through electrostatic attraction. The adsorption performance was strongly affected by solution pH and ionic strength. Adsorption isotherm of HA on PA-NH₂ can

be well described by Freundlich model and adsorption kinetics can be fitted by pseudo-second order kinetics. The present results highlight that PA-NH₂ is one of available candidate adsorbents for the removal of HA from water and wastewater.

Acknowledgements

This work was supported by National Science Foundation of China (21677092), Innovation Program of Scientific Research Group of Shaanxi Province (2014KCT-15), and the Scientific Research Program Funded by Shaanxi Provincial Education Department (15JK1095), Xi'an, China.

References

- [1] C. Li, Y. Dong, D. Wu, L. Peng, H. Kong, Surfactant modified zeolite as adsorbent for removal of humic acid from water, *Appl. Clay Sci.*, 52 (2011) 353–357.
- [2] Y.L. Thuyavan, N. Anantharaman, G. Arthanareeswaran, A.F. Ismail, Adsorptive removal of humic acid by zirconia embedded in a poly(ether sulfone) membrane, *Ind. Eng. Chem. Res.*, 53 (2014) 11355–11364.
- [3] C. Shuang, F. Pan, Q. Zhou, A. Li, P. Li, W. Yang, Magnetic polyacrylic anion exchange resin: Preparation, characterization and adsorption behavior of humic acid, *Ind. Eng. Chem. Res.*, 51 (2011) 4380–4387.
- [4] X. Zhang, R.A. Minear, Characterization of high molecular weight disinfection byproducts resulting from chlorination of aquatic humic substances, *Environ. Sci. Technol.*, 36 (2002) 4033–4038.
- [5] C. Dong, W. Chen, C. Liu, Preparation of novel magnetic chitosan nanoparticle and its application for removal of humic acid from aqueous solution, *Appl. Surf. Sci.*, 292 (2014) 1067–1076.
- [6] S. Capasso, S. Salvestrini, E. Coppola, A. Buondonno, C. Colella, Sorption of humic acid on zeolitic tuff: A preliminary investigation, *Appl. Clay Sci.*, 28 (2005) 159–165.
- [7] E.A. Ghabbour, G. Davies, K. O'Donoghuy, T.L. Smith, M.E. Goodwillie, Adsorption of a plant- and a soil-derived humic acid on the common clay kaolinite, in G. Davies & E. A. Ghabbour (Eds.), *Humic substances*, Woodhead Publishing, 1 (1998) 185–194.
- [8] E.A. Ghabbour, G. Davies, M.E. Goodwillie, K. Donaghay, T. L. Smith, Thermodynamics of peat-, plant-, and soil-derived humic acid sorption on kaolinite, *Environ. Sci. Technol.*, 38 (2004) 3338–3342.
- [9] M. Salman, B. El-Eswed, F. Khalili, Adsorption of humic acid on bentonite, *Appl. Clay Sci.*, 38 (2007) 51–56.
- [10] C. Leodopoulos, D. Doulia, K. Gimouhopoulos, T.M. Triantis, Single and simultaneous adsorption of methyl orange and humic acid onto bentonite, *Appl. Clay Sci.*, 70 (2012) 84–90.
- [11] X. Feng, A.J. Simpson, M.J. Simpson, Chemical and mineralogical controls on humic acid sorption to clay mineral surfaces, *Org. Geochem.*, 36 (2005) 1553–1566.
- [12] M. Wang, L. Liao, X. Zhang, Z. Li, Adsorption of low concentration humic acid from water by palygorskite, *Appl. Clay Sci.*, 67–68 (2012) 164–168.
- [13] G. Lv, X. Wang, L. Liao, Z. Li, M. He, Simultaneous removal of low concentrations of ammonium and humic acid from simulated groundwater by vermiculite/palygorskite columns, *Appl. Clay Sci.*, 86 (2013) 119–124.
- [14] S. Deng, R.B. Bai, Aminated polyacrylonitrile fibers for humic acid adsorption: Behaviors and mechanisms, *Environ. Sci. Technol.*, 37 (2003) 5799–5805.
- [15] X. Zhang, R. Bai, Mechanisms and kinetics of humic acid adsorption onto chitosan-coated granules, *J. Colloid Interf. Sci.*, 264 (2003) 30–38.

- [16] W. Ngah, S. Fatinathan, N. Yosop, Isotherm and kinetic studies on the adsorption of humic acid onto chitosan- H_2SO_4 beads, *Desalination*, 272 (2011) 293–300.
- [17] Y. Tang, S. Liang, S. Yu, N. Gao, J. Zhang, H. Guo, Y. Wang, Enhanced adsorption of humic acid on amine functionalized magnetic mesoporous composite microspheres, *Colloids Surf. A*, 406 (2012) 61–67.
- [18] T. Anirudhan, P. Suchithra, S. Rijith, Amine-modified polyacrylamide–bentonite composite for the adsorption of humic acid in aqueous solutions, *Colloids Surf. A*, 326 (2008) 147–156.
- [19] J. Wang, L. Bi, Y. Ji, H. Ma, X. Yin, Removal of humic acid from aqueous solution by magnetically separable polyaniline: Adsorption behavior and mechanism, *J. Colloid Interf. Sci.*, 430 (2014) 140–146.
- [20] J. Wang, X. Han, H. Ma, Y. Ji, L. Bi, Adsorptive removal of humic acid from aqueous solution on polyaniline/attapulgite composite, *Chem. Eng. J.*, 173 (2011) 171–177.
- [21] R.G. Acres, A.V. Ellis, J. Alvino, C.E. Lenahan, D.A. Khodakov, G.F. Metha, G.G. Andersson, Molecular structure of 3-aminopropyltriethoxysilane layers formed on silanol-terminated silicon surfaces, *J. Phys. Chem. C*, 116 (2012) 6289–6297.
- [22] Y. Chen, Y. Zhao, S. Zhou, X. Chu, L. Yang, W. Xing, Preparation and characterization of polyacrylamide/palygorskite, *Appl. Clay Sci.*, 46 (2009) 148–152.
- [23] Q. Tao, Z. Xu, J. Wang, F. Liu, H. Wan, S. Zheng, Adsorption of humic acid to aminopropyl functionalized SBA-15, *Micropor. Mesopor. Mater.*, 131 (2010) 177–185.
- [24] M. Jones, N. Bryan, Colloidal properties of humic substances, *Adv. Colloid Interface Sci.*, 78 (1998) 1–48.
- [25] J. Duan, F. Wilson, N. Graham, J.H. Tay, Adsorption of humic acid by powdered activated carbon in saline water conditions, *Desalination*, 151 (2003) 53–66.
- [26] J. Wang, Y. Zhou, A. Li, L. Xu, Adsorption of humic acid by bi-functional resin JN-10 and the effect of alkali-earth metal ions on the adsorption, *J. Hazard. Mater.*, 176 (2010) 1018–1026.
- [27] N.M. O’Boyle, A.L. Tenderholt, K.M. Langner, Cclib: A library for package-independent computational chemistry algorithms, *J. Comput. Chem.*, 29 (2008) 839–845.
- [28] A. Xue, S. Zhou, Y. Zhao, X. Lu, P. Han, Effective NH_2 -grafting on attapulgite surfaces for adsorption of reactive dyes, *J. Hazard. Mater.*, 194 (2011) 7–14.
- [29] T. Jesionowski, A. Krysztalkiewicz, Influence of silane coupling agents on surface properties of precipitated silicas, *Appl. Surf. Sci.*, 172 (2001) 18–32.

Supporting Information

Table S1
Simulated parameters from Langmuir and Freundlich model for HA adsorption onto PA-NH₂

Model	Simulated parameters	
Langmuir model	q_m (mg/g)	71.43
	b (L/mg)	0.118
	R^2	0.941
Freundlich model	K_f	14.42
	n	2.74
	R^2	0.992

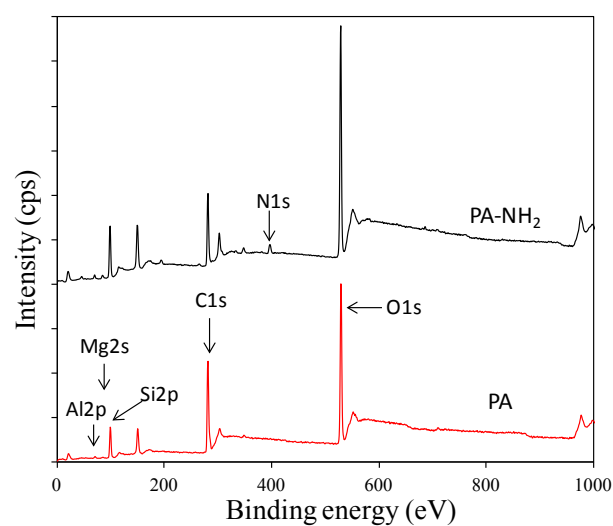


Fig. S1. The survey XPS spectra of PA and PA-NH₂.

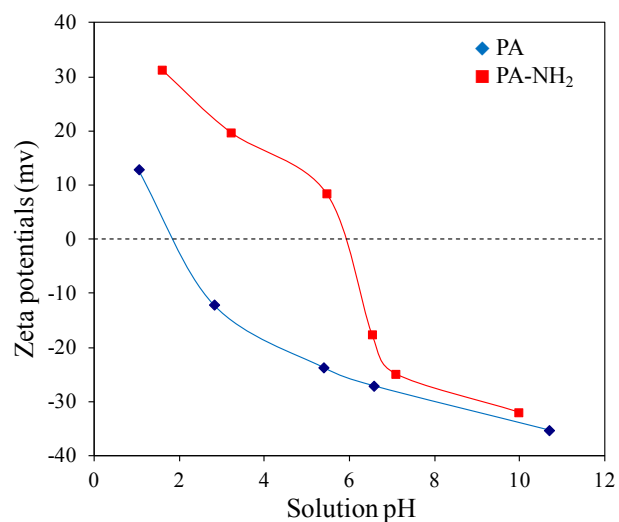


Fig. S2. Zeta potentials of PA and PA-NH₂.

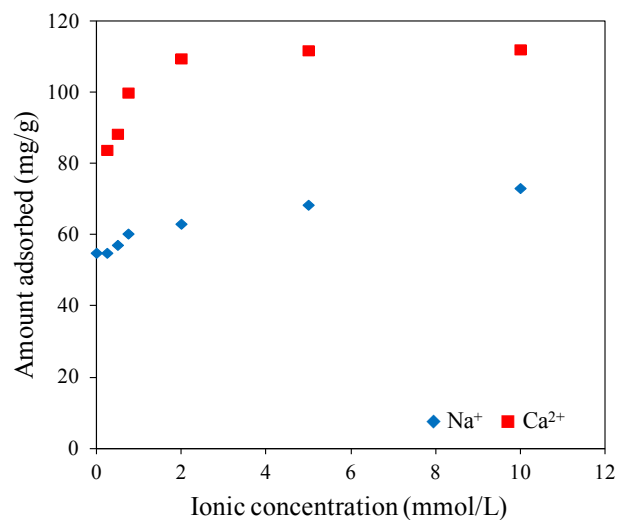


Fig. S3. Effect of Na⁺ and Ca²⁺ with different concentration on HA adsorption on PA-NH₂.